

Performance of Beam Diagnostics for SPring-8 Linac

K. Yanagida, S. Suzuki, H. Yoshikawa, T. Hori, A. Mizuno, K. Tamezane, M. Koderu and H. Yokomizo
 JAERI-RIKEN SPring-8 Project Team
 JAERI, Tokai-mura, Naka-gun, Ibaraki-ken, 319-11, Japan

Abstract

A non-destructive current monitor and a destructive emittance monitor are developed for SPring-8 linac. A wall current monitor has a fast rise time of ~ 250 ps, an output of ~ 1.4 V/A (effective resistance of 1.4Ω), a linearity within 2.2% in the current range of 0-10A and a broad bandwidth (20kHz-2GHz). Transverse emittances were successfully measured using slits and profile monitors (wire grid monitors). The emittance monitor has a geometrical resolution of 0.3mm for X,Y and of ~ 0.1 mrad for X',Y'. The signal processor for the wire grid monitor has a sensitivity of 0.83pC/pulse. A secondary emission rate is obtained as $\sim 10\%$.

I. INTRODUCTION

In the electron linac, principal beam characteristics such as beam current, emittance and energy deviation are determined by the beam dynamics from the gun to the point where the beam energy is several MeV. The preinjector (Fig.1) was constructed to examine the beam characteristics as a part of SPring-8 (Super Photon ring 8 GeV) linac. A beam test started from August 1992, and the commissioning is under way [1]. In the preinjector several monitors are installed not only to measure the beam characteristics but also to examine the performance of monitors using the electron beam. This article presents the performance of a short pulse current monitor (SCM, a wall current monitor) and a transverse emittance monitor (Slit1 and a wire grid monitor). The overall description of diagnostics in SPring-8 linac and of each monitors are given in the previous papers [2] [3].

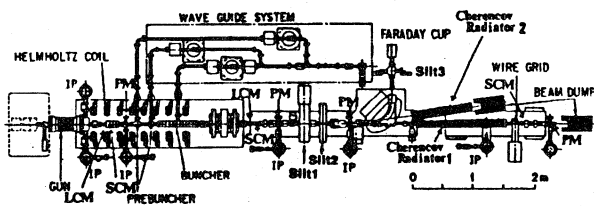


Fig.1. Arrangement of the preinjector.

There are two wall current monitors are installed in the preinjector. In order to measure the performance of gun one is placed at the exit of gun. Another is placed at the exit of buncher to obtain a transmission rate of the bunching section.

II. WALL CURRENT MONITOR

A. Structure of Wall Current Monitor

The preinjector generates a nanosecond electron beam which is required to provide a single bunch in the storage ring.

It is essential to know the peak current and the pulse width (waveform). A monitor is required to have a rise time of ≤ 300 ps. It is well known a wall current monitor has a fast rise time [4], while the fast current transformer with an amorphous core was developed [5]. However in SPring-8 linac a wall current monitor (Fig.2) was designed with careful considerations. It was tested using the spectrum analyzer and using the electron beam as follows.

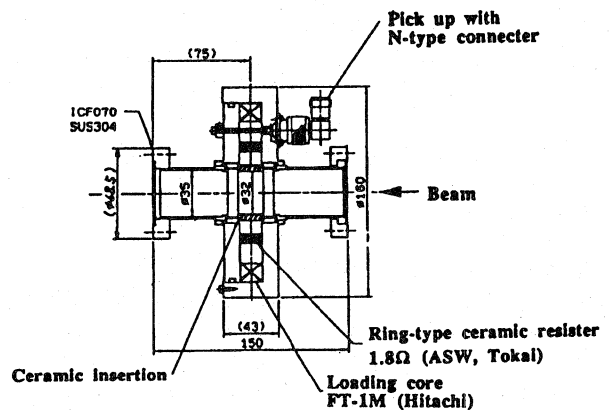


Fig.2. Cross section of the wall current monitor.

The wall current monitor is composed of a ring-type ceramic resistor (ASW, TOKAI) with nominal resistance of 1.8Ω connected across a ceramic insertion, a signal pick up and loading core (FT-1M, HITACHI). The pick up detects voltage emerging on the resistor, however it also consists a single turn coil surrounding the core. For this reason this current monitor is regarded not only as a wall current monitor but also as a current transformer. A signal is transported by 20m long WF cable and observed by the transient recorder (SCD5000, TEKTRONIX).

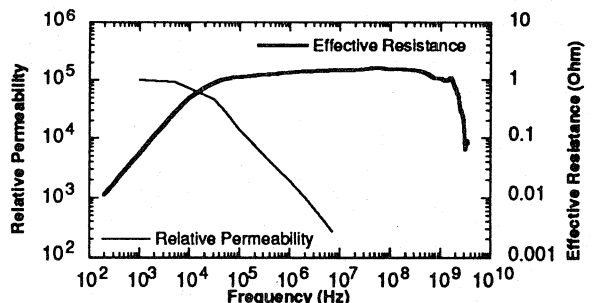


Fig.3. Frequency spectrum of the effective resistance and relative permeability of the core.

B. Frequency Spectrum

A frequency spectrum is obtained by feeding RF power using tapered pipe and inner conductor instead of the beam [2]. Fig.3 shows the frequency spectrum of the effective resistance and the relative permeability of the core. The effective resistance means the output voltage per 1 Ampere pulse (V/A). A resistance of flat top is $\sim 1.4\Omega$ and the frequency region above 0.7Ω is 20kHz-2GHz (bandwidth). While the relative permeability decreases as f^{-1} above 20kHz. This means the bandwidth is determined by the core's characteristic.

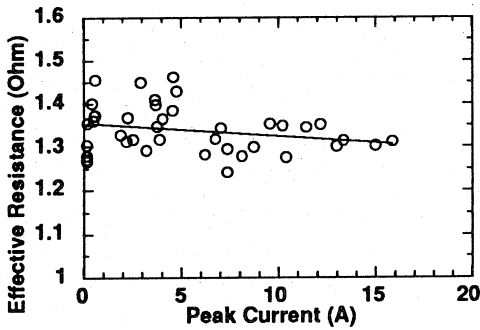


Fig.4. Reduction of the effective resistance. Circles are measured, and the line is linear fitting.

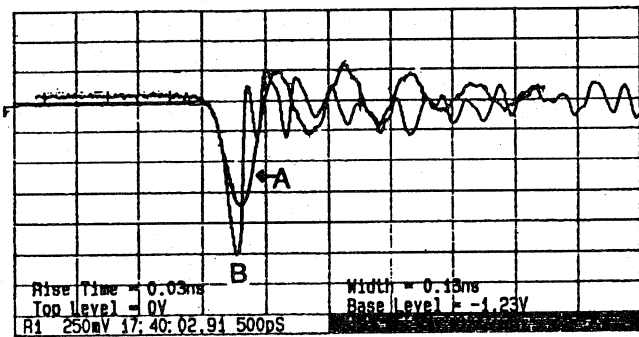


Fig.5. Waveform of the single bunched beam (after buncher, 500ps/div.), A is wall current monitor's (45mA/div.), B is coaxial Faraday cup's (10mA/div.).

C. Linearity of Output

A linearity of output is not preserved when the beam current becomes higher because of core's saturation. The linearity is expressed by the decrease of effective resistance at the higher beam current. The effective resistances were measured using the electron beam. The wall current monitor and the long pulse current monitor (2100 PEARSON, which is well calibrated) are placed in the beam line side by side. The peak voltage of 40ns beam were measured by both monitors. Here we assume the beam currents are obtained correctly by the long pulse current monitor. The effective resistances are obtained so that the peak voltages of the wall current monitor's are divided by the peak currents. Fig.4 is the effective resistance versus peak current. At $\sim 0A$ the effective resistance is $\sim 1.36\Omega$ which agrees to the value from frequency spectrum. But the effect of core's saturation appeared, because

the effective resistance is reduced by 2.2% at the beam current of 10A.

D. Rise Time

Fig.5 is the waveforms of a single bunched beam. If a pulse width of the beam generated by the gun is shorter than 350ps, which is the period of acceleration frequency, the shingle bunched beam can be produced. These waveforms were measured by the wall current monitor placed after the buncher and by the coaxial Faraday cup placed after the beam extraction window in the air. Thus the beam is bunched very short, the input pulse is regarded like as a delta function. The waveform A shows the rise time of $\sim 250ps$. But the waveform B shows the rise time of $\sim 100ps$, which is thought as the rise time of the WF cable ($-3dB$, at 3GHz). So the rise time of the wall current monitor is thought to be shorter than 250ps.

III. EMITTANCE MONITOR

A. Structure of Emittance Monitor

Emittances were measured using slits and wire grid monitors [6] [7]. The phase space is scanned directly. A width and a thickness of the slit are 0.3mm and 30mm respectively. The wire grid monitor has a single tungsten wire with a diameter of 0.3mm. Electrons produce secondary emission in passing through the wire, and positive charge is deposited on it. The wire grid monitor also has two electrode wires to absorb the secondary emission. The distance from the slits to the wire grid monitors is 3.34m. This geometry provides the geometrical resolution of 0.3mm for X,Y and of $\sim 0.1mrad$ for X',Y'.

B. Charge Sensitive Amplifier

A charge sensitive amplifier is developed for the signal processing (Fig.6). An expected charge is $1pC \sim 0.1\mu C$ /pulse in the operation. A maximum sensitivity is designed as $\sim 1V/pC$.

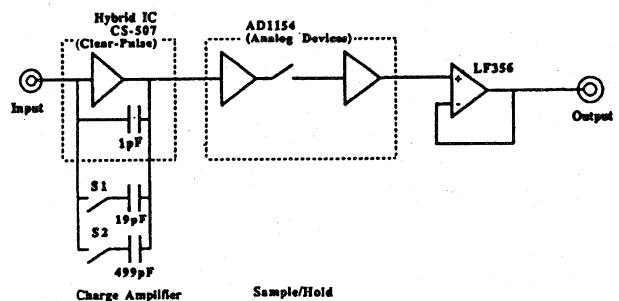


Fig.6. Block diagram of the charge sensitive amplifier with the hybrid IC.

The charge sensitive amplifier consists of the hybrid-IC (CS-507, CLEAR-PULSE) and the sample/hold IC (AD1154, ANALOG DEVICES). The CS-507 has a sensitivity of $1V/pC$ nominally. And the sensitivity can be decreased by attaching extra capacitors. The sensitivities are measured as $0.83V/pC$, $44V/nC$ and $2V/nC$. The sample/hold IC (AD1154) is

prepared for the data acquisition by VME module because an analog DC output is requested.

B. Emittance Measurement

Because of large beam size slits and wire grid monitors were moved by 1mm step. Typical charge distribution is shown in Fig.7, at the beam condition of 1ns pulse width, 4.7A peak current. After data processing, the emittance ellipses are obtained (Fig.8). Each ellipse is discriminated by percentage of beam. Charge density is summed up in the all phase space to obtain the total charge. Percentage of the beam results from a summation over all charge density within the ellipse, divided by the total charge [8]. Table 1 shows emittances in various pulse modes.

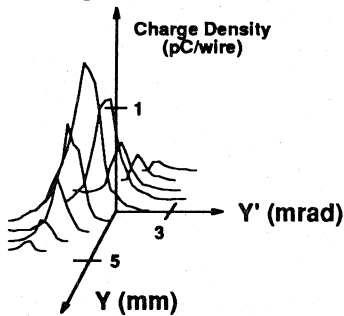


Fig.7. Charge distribution in phase space Y-Y' at 1ns beam.

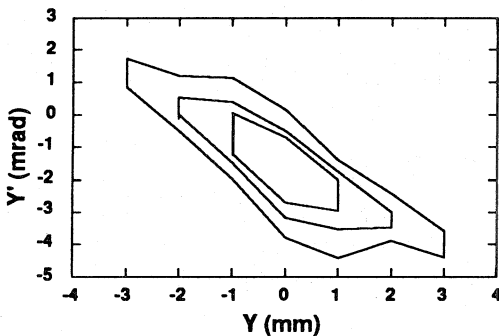


Fig.8. Emittance ellipses. Inner to outer ellipses correspond to 50,70 and 90% emittance ellipses.

Table 1
Measured Emittances

Pulse Mode and Direction	Peak Current (A)	Emittance (90%, $\pi\text{mm}\cdot\text{mrad}$)	Normalized Emittance (90%, $\pi\text{mm}\cdot\text{mrad}$)
1ns-X	4.7	5.2	122
1ns-Y	4.7	4.5	106
1ns-X	7.1	5.1	120
1ns-Y	7.1	8.6	202
1 μs -X	0.06	5.1	100
1 μs -Y	0.06	6.8	133

C. Secondary Emission Rate

The monitor is based on secondary emission from the wire as the incident electron beam impinges on it. The number of

secondaries is proportional to the primaries. In our study the secondary emission rate is measured as $\sim 10\%$ using the wire of 0.3mm diameter at an energy of ~ 10 MeV taking account of geometrical interception. On the other hand, the secondary emission rate is reported as 3-3.5 % at the beam energy of 30-1000 MeV using the wire of 0.1 mm diameter [9]. Because the secondary emission rate is proportional to surface area of wire, both values are thought agreed.

IV. CONCLUSION AND DISCUSSION

The wall current monitor was developed for the nanosecond beam. It provides the fast rise time of $\sim 250\text{ps}$, the linearity within 2.2% in the current range of 0-10A, the effective resistance of $\sim 1.4\Omega$ and the band width from 20kHz to 2GHz. By the study of this type of monitor we understood relations between design parameters and performances; for example, rise time and resonant frequency of the monitor, bandwidth and core's characteristic, linearity and volume of the core, effective resistance and nominal resistance. With the knowledge of these natures, we will develop the new higher performance monitor.

The emittance monitor for the lower energy beam (10-60MeV) was developed. It consists of slits and wire grid monitors. The emittance monitor has a geometrical resolution of 0.3mm and $\sim 0.1\text{mrad}$ respectively. The signal processor for the wire grid monitor has a maximum sensitivity of 0.83pC/pulse. A secondary emission rate is obtained as $\sim 10\%$. In the higher energy region (at the energy of 1GeV) three multi-wire grid monitors will be used to measure emittance. The charge sensitive amplifier was developed as a prototype of multi-channel amplifier.

V. REFERENCES

- [1] S.Suzuki, et al., "Initial Data of Linac Preinjector for SPring-8." in Proc. of '93 PAC, Washington D.C., May 1993, to be published.
- [2] K.Yanagida, et al., "Development of Beam Diagnostics for SPring-8 Linac." in Proc. of '92 Linear Acc. Conf., Ottawa, Ontario, Aug. 1992, pp. 665-667.
- [3] K.Yanagida, et al., "Beam Monitors for SPring-8 Linac." Proc. of 16th Linear Acc. Meeting, Tokyo, Sept. 1991, pp. 269-271.
- [4] R.F.Koonz and R.H.Miller, "Nanosecond Electron Beam Generation and Instrumentation at SLAC." IEEE Trans. Nucl. Sci., Vol. NS-22, No.3, June 1975, pp. 1350-1353.
- [5] T.Kobayashi, et al., "Development of A Beam Current Monitor by Using Amorphous Core (IV)." Proc. of 17th Linear Acc. Meeting, Sendai, Sept. 1992, pp. 210-212.
- [6] H.Koziol, "Beam Diagnostics." CERN 89-05, 1989, pp. 63-101.
- [7] T.Nalanishi, "Measurement of Emittances and Momentum Spectra of A 20 MeV Electron Linac Beam." Nucl. Instr. and Meth., A277,1989, pp. 313-318.
- [8] P.Strehl, "Beam Diagnostics." CERN 87-10, 1987, pp. 99-134.
- [9] R.Chehab, et al., "A Multiwire Secondary Emission Profile Monitor." IEEE Trans. Nucl. Sci., Vol. NS-32, No.5, Oct. 1985, pp. 1953-1355.